An AIE-Active Probe for Detection and Bioimaging of pH Values Based on Lactone Hydrolysis Reaction

Qiao Li
Hainan Normal University
Zhigang Niu
Hainan Normal University
Xuying Nan
Hainan Normal University
Enju Wang (enjuwang@163.com)
Hainan Normal University https://orcid.org/0000-0001-5014-6989

Research Article

Keywords: Fluorescent pH probe, Aggregation-induced emission, Coumarin, Lactone hydrolysis, Cell imaging

Posted Date: March 29th, 2022

DOI: https://doi.org/10.21203/rs.3.rs-1458998/v1

Abstract

Cellular pH homeostasis is essential for many physiological and pathological processes. pH monitoring is helpful for the diagnosis, treatment and prevention of disorders and diseases. Herein, we developed a ratiometric fluorescent pH probe (TCC) based on a coumarin derivative containing a highly active lactone ring. TCC exhibited a typical AIE effect and emitted blue fluorescence under weak acidic condition. When under weak basic condition, the active lactone moiety underwent a hydrolysis reaction to afford a water-soluble product, which gave red-shifted emission. The emission color change from blue through cyan and then to yellow within pH 6.5–9.0 which is approximate to the biological pH range. And the fluorescence color change along with pH value is reversible. Furthermore, TCC was successfully utilized in the detection of the intracellular pH change of live HeLa cells, which indicated that TCC had practical potential in biomedical research.

Introduction

Various biological microenvironments take on specific pH ranges. For instance, the extracellular fluid is slightly alkaline at about pH 7.4, the cytoplasm is at near-neutral pH 7.2, whereas the lysosome pH is in an acidic range of pH 4.5–5.0. The pH homeostasis plays an extremely important role in many biological processes, such as cell proliferation and apoptosis [1], ion transport and homeostasis [2], cellular transport and signal transduction [3, 4]. Slight pH fluctuation may cause injury to cells and give rise to disease, such as stroke and Alzheimer's diseases [5, 6]. For cancer cells, the extracellular acidosis and intracellular alkalization is a common characteristic. The prevention of intracellular pH increases by inhibiting ion transporter may be an effective therapeutic approach for cancers [7]. Hence, it is of great significance for human body health to monitor biological pH fluctuation. Among various approaches for measuring pH, fluorescence probe technology has aroused wide attention due to their high sensitivity, reversibility and visual response. Above all, it is noninvasive, and can be utilized in real-time observation of the pH fluctuation by confocal fluorescence microscopy.

In general, an excellent probe for biological detection should meet the following requirements: (1) *highly water solubility* Most organic luminophores are poorly soluble in water, so they are not applicable for utilization in biological aqueous media [8 – 11]; (2) *good luminescent stability* Many fluorescence probes based on aromatic luminophores suffer from the aggregation-caused quenching (ACQ) effect that limited their broad applications in bioassays [12]; (3) *high sensitivity in biological pH range* The biological pH range is usually 6.5 to 8 except for the acidic lysosome [13]. A pH bioprobe should give obvious emission color changes within the pH range [14–21], instead of just the variations of the emission intensity [22–25]. For the pH probes based on the conventional organic luminophores, it's hard to satisfy all of the above conditions [26–28]. Fortunately, the discovery of aggregation-induced emission (AIE) gives an opportunity to meet these requirements. The AIE-based fluorescent probes have been widely used in bioassays due to their good biocompatibility, high photostability and large Stokes shift [29–32].

Herein, a new fluorescence probe abbreviated as TCC, was readily synthesized via the Knoevenagel reaction between 5-*tert*-butyl-2-hydroxyisophthalaldehyde and malononitrile followed by an intramolecular nitrile-phenol condensation reaction in total 80% yield [33]. It worked well in water, displayed excellent AIE effect and showed sensitive fluorescence responses to pH variation in near neutral pH range. The fluorescence probe operated via a pH-dependent and reversible ring-opening reaction of the lactone moiety which resulted in an obvious fluorescence change from blue through cyan and then to yellow within the biological pH range. Furthermore, the study on the utilization in the live cell fluorescence imaging showed its excellent performance in the real-time monitoring of the intracellular pH values. The synthetic route and its pH-dependent structure transformation were shown in Scheme 1.

Experimental

Reagents and Apparatus

All chemicals were obtained from commercial suppliers. ^{1}H NMR and ^{13}C NMR spectra were recorded on a Bruker Av400 NMR spectrometer. ESI-MS spectra were performed on a Bruker Esquire HCT mass spectrometer. Fluorescence spectra were taken on a Hitachi F-7000 fluorescence spectrometer. The X-ray diffraction data was collected on an Agilent Gemini A Ultra diffractometer. Images of cells were obtained using a Nikon A1 confocal laser scanning microscope.

Synthesis of TCC

A mixture of 5-*tert*-butyl-2-hydroxyisophthalaldehyde (0.21 g, 1 mmol), ammonium acetate (0.17 g, 2.2 mmol), glacial acetic acid (1 ml) and malononitrile (0.15g, 2.2 mmol) was heated to 65°C for 3 h. After cooling to room temperature, 5 mL water was added to the reaction mixture under stirring, and then a yellow precipitate appeared. After purified by means of silica gel chromatograph using chloroform as the eluent, TCC was obtained as light yellow powder (0.24 g, 80%). ^{1}H NMR (400 MHz, DMSO-d_6) δ: 8.95 (s, 1H), 8.78 (s, 1H), 8.48 (d, 1H, J = 2.0 Hz), 8.12 (d, 1H, J = 2.0 Hz), 1.36 (s, 9H). ^{13}C NMR (100 MHz, DMSO-d_6) δ 155.7, 153.9, 153.2, 150.1, 147.8, 131.6, 131.4, 119.3, 117.8, 114.2, 113.4, 112.8, 103.0, 86.8, 34.8, 30.6. ESI-MS m/z calculated for [M + AcO^-] 362.1, found 362.2 (Fig. S1 – 3).

Results And Discussion

Crystal Structure

Colorless sheet-like crystals of TCC suitable for X-ray analysis were obtained by slowly evaporating its tetrahydrofuran solution at room temperature. The crystal data were provided in supplementary material (Table S1). For more information, see the crystallographic information file that has been deposited in the Cambridge Crystallographic Data Centre (CCDC 2131284). It crystallizes in the monoclinic space group $P2_1/c$. As shown in Fig. 1(a), the molecule adopts a twisted conformation with dihedral angles of 31.4° between the coumarin moiety and the methylenemalononitrile moiety, indicating weak conjugation

between them. Thus, in solvent the two groups would undergo active intramolecular rotation, which effectively dissipates the excited-state energy of TCC and leads to nonradiative relaxation. But in its aggregate state the intramolecular rotational movement is restricted, which is a positive factor for the radiative relaxation. Thanks to the twisted conformation and the steric effect of *tert*-butyl group, no *π*-*π* stacking interaction was observed in the crystals of TCC (Fig. 1b). Hence, TCC has huge potential to be an AIE-active luminogen.

Fluorescence properties

In exploring the photoluminescence of TCC, it was accidentally found that its fluorescence behaviors are sensitively dependent on the pH values. When under acidic condition, TCC displays good AIE activity. The AIE performance of TCC in DMSO/H_2O at pH 5 was shown in Fig. 2a. TCC in DMSO was nearly non-fluorescent. A gradual emission enhancement was observed in initial stage of raising water content of the DMSO/H_2O mixed solvent. When the water volume fraction (f_w) was over 90%, the fluorescence underwent a rapid intensity enhancement. Figure 2b showed a 15-fold increased emission intensity when the volume fraction of water goes from 0 to 99.9%. The excellent AIE performance in organic solvent-free water ensured the utilization of TCC in biological aqueous media. When under alkaline condition, TCC is non-AIE-active due to its high water solubility, but exhibits a significant fluorescence redshift from 440 nm to 560 nm as shown in Fig. 3a. It should be noted that some incubation time is necessary for the redshift of the fluorescence emission. The effect of pH on incubation time at 25°C was show in Fig. 3b. Obviously, it took less time to reach the fluorescence emission peaks at pH 10 than at pH 8, and the emission peaks at pH 10 was higher than that at pH 8. The pH-dependent incubation time implied that an OH^--promoted reaction possibly occurred. The ESI-MS analysis indicated that TCC underwent a lactone hydrolysis reaction affording the product TCHC (Scheme 1), which was affirmed by the peak at m/z 319.6 for $[M-H]^-$ and 275.7 for $[M-CO_2-H]^-$ (calculated for [M-H]– 320.1 and $[M-CO_2-H]^-$ 276.1, Fig. S4).

pH detection

The pH-dependent fluorescence of TCC makes it possible to detect pH values. For inspecting its pH-responsive performance, the fluorescence spectra in PBS buffer with different pH were measured and shown in Fig. 4a. When pH increased from pH 4 to pH 10, the peak emission at 440 nm gradually weakened, and a new peak at 560 nm appeared when excited at 320 nm. An isoemissive point appeared at pH 7.6 which is very close to the physiological pH range indicating the potential of TCC as an applicable pH indicator in biosystems (Fig. 4b). The emission at 560 nm is much weaker than that at 440 nm because the excitation wavelength (320 nm) is so short for the emission at 560 nm. When under alkaline condition, it should be excited at 450 nm which can lead to a higher emission intensity at 560 nm (Fig. 3a). As shown in Fig. 4c, an obvious emission color changed from blue through cyan and then to yellow was observed when the pH increased from pH 6.5 to pH 9. Furthermore, the color variances mainly occurred about at pH 7.0 to pH 8.0, which further confirmed its utility value as a pH bioprobe. The reversibility of the pH response was investigated by modulating the pH value of TCC solution between pH

6 and pH 9 alternately and recording the maximum emission intensities respectively (Fig. 4d). It was found that the probe still operated well after undergoing four basic-acidic pH cycles.

Fluorescence imaging

The excellent pH-responsive performance of TCC motivated us to investigate its utilization in intracellular imaging. HeLa cells were incubated with 10 μM TCC for 10 min and then immersed in 20 mmol/L PBS buffer at different pH value for 20 min. The cell samples at different pH values were scanned in green channel and red channel respectively using confocal laser scanning fluorescence microscopy. As shown in Fig. 5, the green fluorescence in HeLa cells gradually got darker with the increase of pH value from 6.0 to 8.0, and even could not be distinguished at pH 9.0. Whereas, higher pH values were helpful to the red fluorescence. At pH 8, the red fluorescence started to appear. When the pH reached 9, a bright red channel image could be observed. Consequently, TCC is capable of detecting the intracellular pH values.

Conclusion

In conclusion, we have developed a fluorescent probe (TCC) containing a pH-dependent lactone ring which would be hydrolyzed to afford a water-soluble product (TCHC) under weak basic condition. TCC exhibited AIE activity and emitted blue fluorescence at about 430 nm, while TCHC emitted yellow fluorescence at about 560 nm. The fluorescence color change along with the dynamic pH change is reversible. Furthermore, TCC was successfully utilized for intracellular pH imaging.

Declarations

Supplementary Information The online version contains supplementary material available at https://

Funding This work is financially supported by the National Natural Science Foundation of China (22061016) and Program for Innovative Research Team in University (IRT-16R19).

Conflicts of Interest/Competing Interests The authors have no conflicts of interest to declare that are relevant to the content of this article.

Ethical Approval Not applicable.

Consent to participate Not applicable.

Consent for publication Not applicable.

Availability of data and material/ Data availability The crystallographic information files that have been deposited in the Cambridge Crystallographic Data Centre (CCDC 2131284) which are freely available for all. The link for CCDC: https://www.ccdc.cam.ac.uk/.

Code Availability not applicable.

Author Contributions EW contributed to the study conception and design, and was the major contributor in writing the manuscript. The synthesis, spectrum test, data analysis and so on were performed by QL with the assistance of XN. The X-ray diffraction data collection and structure determination was performed by ZN.

References

1. Lagadic-Gossmann D, Huc L, Lecureur V (2004) Alterations of intracellular pH homeostasis in apoptosis: origins and roles. Cell Death Differ 11:953–961. https://doi.org/10.1038/sj.cdd.4401466
2. Donoso P, Beltrán M, Hidalgo C (1996) Luminal pH regulates calcium release kinetics in sarcoplasmic reticulum vesicles. Biochemistry 35:13419–13425. https://doi.org/10.1021/bi9616209
3. Neuhoff S, Ungell AL, Zamora I, Artursson P (2003) pH-dependent bidirectional transport of weakly basic drugs across Caco-2 monolayers: implications for drug-drug interactions. Pharm Res 20:1141–1148. https://doi.org/10.1023/A:1025032511040
4. Kullas AL, Martin SJ, Davis D (2007) Adaptation to environmental pH: integrating the Rim101 and calcineurin signal transduction pathways. Mol Microbiol 66:858–871. https://doi.org/10.1111/j.1365-2958.2007.05929.x
5. Wen Y, Zhang W, Liu T, Huo F, Yin C (2017) Pinpoint diagnostic kit for heat stroke by monitoring lysosomal pH. Anal Chem 89:11869–11874. https://doi.org/10.1021/acs.analchem.7b03612
6. Davies TA, Fine RE, Johnson RJ, Levesque CA, Rathbun WH, Seetoo KF, Smith SJ, Strohmeier G, Volicer L, Delva L (1993) Non-age related differences in thrombin responses by platelets from male patients with advanced Alzheimer's disease. Biochem Biophys Res Commun 194:537–543. https://doi.org/10.1006/bbrc.1993.1853
7. White KA, Grillo-Hill BK, Barber DL (2017) Cancer cell behaviors mediated by dysregulated pH dynamics at a glance. J Cell Sci 130:663–669. https://doi.org/10.1242/jcs.195297
8. Chao J, Liu Y, Sun J, Fan L, Zhang Y, Tong H, Li Z (2015) A ratiometric pH probe for intracellular pH imaging. Sens Actuat B-Chem 221:427–433. https://doi.org/10.1016/j.snb.2015.06.087
9. Chen S, Qiu R, Yu Q, zhang X, Wei M, Dai Z (2018) Boranil dyes bearing tetraphenylethene: synthesis, AIE/AIEE effect properties, pH sensitive properties and application in live cell imaging. Tetra Lett 59:2671–2678. https://doi.org/10.1016/j.tetlet.2018.05.081
10. Lin B, Wei Y, Hao Y, Shuang E, Shu Y, Wang J (2021) β-Naphthothiazolium-based ratiometric fluorescent probe with ideal p*K*a for pH imaging in mitochondria of living cells. Talanta 232:122475. https://doi.org/10.1016/j.talanta.2021.122475
11. Wang J, Liu H, Wu M, Liu X, Sun H, Zheng A (2019) Water-soluble organic probe for pH sensing and imaging. Talanta 205:120095. https://doi.org/10.1016/j.talanta.2019.06.095
12. Qian J, Tang BZ (2017) AIE luminogens for bioimaging and theranostics: from organelles to animals. Chem 3:56–91. https://doi.org/10.1016/j.chempr.2017.05.010

13. Mukherjee A, Saha PC, Das RS, Bera T, Guha S (2021) Acidic pH-activatable visible to near-infrared switchable ratiometric fluorescent probe for live-cell lysosome targeted imaging. ACS Sens 6:2141–2146. https://doi.org/10.1021/acssensors.1c00961
14. Zhang XF, Zhang T, Shen SL, Miao JY, Zhao BX (2015) A ratiometric lysosomal pH probe based on the naphthalimide–rhodamine system. J Mater Chem B 3:3260–3266. https://doi.org/10.1039/C4TB02082K
15. Jiao Y, Gong X, Han H, Gao Y, Lu W, Liu Y, Xian M, Shuang S, Dong C (2018) Facile synthesis of orange fluorescence carbon dots with excitation independent emission for pH sensing and cellular imaging. Anal Chim Acta 1042:125–132. https:doi.org/10.1016/j.aca.2018.08.044
16. Yao S, Schafer-Hales KJ, Belfield KD (2007) A new water-soluble near-neutral ratiometric fluorescent pH indicator. Org Lett 9:5645–5648. https://doi.org/10.1021/ol7026366
17. Yang SL, Liu WS, Li G, Bu R, Li P, Gao EQ (2020) A pH-sensing fluorescent metal-organic framework: pH-triggered fluorescence transition and detection of mycotoxin. Inorg Chem 59:15421–15429. https://doi.org/10.1021/acs.inorgchem.0c02419
18. Liu T, Yan B (2020) A stable broad-range fluorescent pH sensor based on Eu^{3+} post-synthetic modification of metal-organic framework. Ind Eng Chem Res 59:1764–1771. https://doi.org/10.1021/acs.iecr.9b06292
19. Liu W, Sun R, Ge JF, Xu YJ, Xu Y, Lu JM, Itoh I, Ihara M (2013) Reversible near-infrared pH probes based on benzo[*a*]phenoxazine. Anal Chem 85:7419–7425. https://doi.org/10.1021/ac4013539
20. Alamry KA, Georgiev NI, El-Daly SA, Taib LA, Bojinov VB (2015) A highly selective ratiometric fluorescent pH probe based on a PAMAM wavelength-shifting bichromophoric system. Spectrochim Acta A 135:792–800. http://dx.doi.org/10.1016/j.saa.2014.07.076
21. Ryan LS, Gerberich J, Haris U, Nguyen D, Mason RP, Lippert AR (2020) Ratiometric pH imaging using a 1,2-dioxetane chemiluminescence resonance energy transfer sensor in live animals. ACS Sens 5:2925–2932. https://doi.org/10.1021/acssensors.0c01393
22. Feng Q, Li Y, Wang L, Li C, Wang J, Liu Y, Li K, Hou H (2016) Multiple-color aggregation-induced emission (AIE) molecules as chemodosimeters for pH sensing. Chem Commun 52:3123–3126. https://doi.org/10.1039/C5CC10423H
23. Wen Y, Zhang W, Liu T, Huo F, Yin C (2017) A pinpoint diagnostic kit for heat stroke by monitoring lysosomal pH. Anal Chem 89:11869–11874. https://doi.org/10.1021/acs.analchem.7b03612
24. Lin B, Fan L, Ying Z, Ge J, Wang X, Zhang T, Dong C, Shuang S, Wong MS (2020) The ratiometric fluorescent probe with high quantum yield for quantitative imaging of intracellular pH. Talanta 208:120279. https://doi.org/10.1016/j.talanta.2019.120279
25. Cao L, Li X, Wang S, Li S, Li Y, Yang G (2014) A novel nanogel-based fluorescent probe for ratiometric detection of intracellular pH values. Chem Commun 50:8787–8790. https://doi.org/10.1039/C4CC03716B
26. WangY, Zeng L, Zhou J, Jiang B, Zhao L, Wang C, Xu B (2019) A dansyl fluorescent pH probe with wide responsive range in aqueous solution. Spectrochim Acta A 223:117348.

https://doi.org/10.1016/j.saa.2019.117348

27. Qiu J, Jiang S, Guo H, Yang F (2018) An AIE and FRET-based BODIPY sensor with large Stoke shift: novel pH probe exhibiting application in CO_3^{2-} detection and living cell imaging. Dyes Pigm 157:351–358. https://doi.org/10.1016/j.dyepig.2018.05.013
28. Peng H, Stolwijk JA, Sun LN, Wegener J, Wolfbeis OS (2010) A nanogel for ratiometric fluorescent sensing of intracellular pH values. Angew Chem Int Ed 49:4246–4249. https://doi.org/10.1002/anie.200906926
29. Yang Z, Qin W, Lam JWY, Chen S, Sung HHY, Williams ID, Tang BZ (2013) Fluorescent pH sensor constructed from a heteroatom-containing luminogen with tunable AIE and ICT Characteristics. Chem Sci 4:3725–3730. https://doi.org/10.1039/C3SC50648G
30. Wang X, Wang H, Niu Y, Wang Y, Feng L (2020) A facile AIE fluorescent probe for broad range of pH detection. Spectrochim Acta A 226:117650. https://doi.org/10.1016/j.saa.2019.117650
31. Shi X, Yan N, Niu G, Sung SHP, Liu Z, Liu J, Kwok RTK, Lam JWY, Wang WX, Sung HHY, Williams ID, Tang BZ In vivo monitoring of tissue regeneration using a ratiometric lysosomal AIE probe.Chem Sci11:3152–3163. https://doi.org/10.1039/C9SC06226B
32. Shi L, Liu Y, Wang Q, Wang T, Ding Y, Cao Y, Li Z, Wei H (2018) A pH responsive AIE probe for enzyme assays. Analyst 143:741–746. https://doi.org/10.1039/C7AN01710C
33. Lakshmi PR, Kumar PS, Elango KP (2020) A simple fluorophore-imine ensemble for colorimetric and fluorescent detection of CN^- and HS^- in aqueous solution. Spectrochim Acta A 229:117974. https://doi.org/10.1016/j.saa.2019.117974

Scheme

Schemes 1 is available in the Supplementary Files section.

Figures

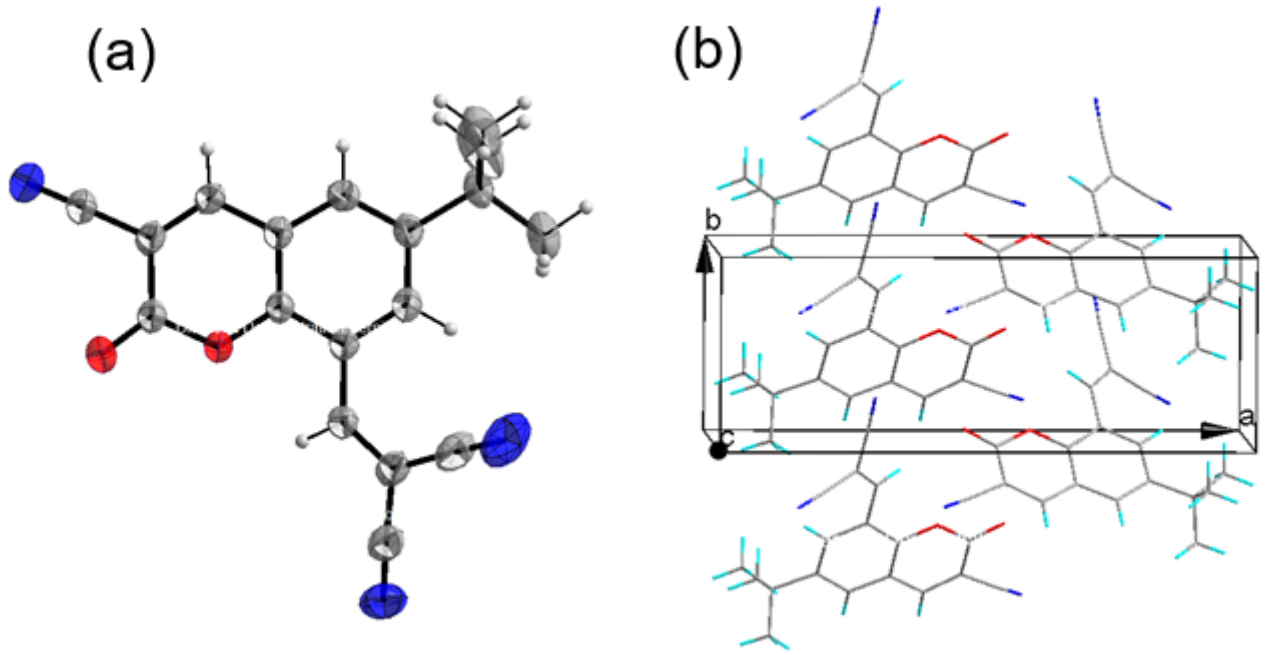

Figure 1

(a) ORTEP drawing of TCC with 50% probability ellipsoids. (b) Crystal packing arrangement along the *b*-axis in which all hydrogen atoms are omitted for clarity.

Figure 2

(a) fluorescence emission spectra of TCC (10 μmol/L) in DMSO/H_2O mixtures with different volume fractions of water (f_w) at pH 5 when excited at 320 nm. (c) Plot of fluorescence intensity versus water fraction.

Figure 3

(a) Fluorescence spectra of TCC (10 μmol/L) at pH 10 in water containing tiny amounts of DMSO when excited at 450 nm. (b) Time-dependent fluorescence emission intensities of TCC (10 μmol/L) at 25 °C and at pH 8 and pH 10 respectively.

Figure 4

(a) Fluorescence responses of 10 μmol/L TCC to different pH values in PBS buffer containing tiny amounts of DMSO under 320 nm excitation. (b) Plots of fluorescence intensity at 440 nm and 560 nm

versus pH values under 320 nm excitation. (c) Fluorescence photographs of TCC at different pH taken in dark-box ultraviolet analyzer under 365 nm excitation. (d) Reversibility of the pH response. The excitation wavelength is 320 nm when pH = 6, and 450 nm when pH = 9 in the reversibility research.

Figure 5

Confocal images of HeLa cells stained with TCC in various pH buffers. HeLa cells were incubated with probe TCC (10μM) for 10 min and then immersed in 20 mmol/L PBS buffers for 20 min at pH 6.0, pH 7.0, pH 8.0 and pH 9.0 respectively. The cell samples at different pH values were scanned in green channel and red channel respectively.

Supplementary Files

This is a list of supplementary files associated with this preprint. Click to download.

- Scheme1.png
- ESI.docx